

# Neoadjuvant versus adjuvant ipilimumab plus nivolumab in macroscopic stage III melanoma

Christian U. Blank<sup>1,2\*</sup>, Elisa A. Rozeman<sup>1,2</sup>, Lorenzo F. Fanchi<sup>2</sup>, Karolina Sikorska<sup>3</sup>, Bart van de Wiel<sup>4</sup>, Pia Kvistborg<sup>2</sup>, Oscar Krijgsman<sup>2</sup>, Marlous van den Braber<sup>2</sup>, Daisy Philips<sup>2</sup>, Annegien Broeks<sup>4</sup>, Johannes V. van Thienen<sup>1</sup>, Henk A. Mallo<sup>1</sup>, Sandra Adriaansz<sup>1</sup>, Sylvia ter Meulen<sup>5</sup>, Loes M. Pronk<sup>3</sup>, Lindsay G. Grijpink-Ongering<sup>3</sup>, Annemarie Bruining<sup>6</sup>, Rachel M. Gittelman<sup>7</sup>, Sarah Warren<sup>8</sup>, Harm van Tinteren<sup>3</sup>, Daniel S. Peeper<sup>2</sup>, John B. A. G. Haanen<sup>1,2</sup>, Alexander C. J. van Akkooi<sup>5</sup> and Ton N. Schumacher<sup>2\*</sup>

**Adjuvant ipilimumab (anti-CTLA-4) and nivolumab (anti-PD-1) both improve relapse-free survival of stage III melanoma patients<sup>1,2</sup>. In stage IV disease, the combination of ipilimumab + nivolumab is superior to ipilimumab alone and also appears to be more effective than nivolumab monotherapy<sup>3</sup>. Preclinical work suggests that neoadjuvant application of checkpoint inhibitors may be superior to adjuvant therapy<sup>4</sup>. To address this question and to test feasibility, 20 patients with palpable stage III melanoma were 1:1 randomized to receive ipilimumab 3 mg kg<sup>-1</sup> and nivolumab 1 mg kg<sup>-1</sup>, as either four courses after surgery (adjuvant arm) or two courses before surgery and two courses postsurgery (neoadjuvant arm). Neoadjuvant therapy was feasible, with all patients undergoing surgery at the preplanned time point. However in both arms, 9/10 patients experienced one or more grade 3/4 adverse events. Pathological responses were achieved in 7/9 (78%) patients treated in the neoadjuvant arm. None of these patients have relapsed so far (median follow-up, 25.6 months). We found that neoadjuvant ipilimumab + nivolumab expand more tumor-resident T cell clones than adjuvant application. While neoadjuvant therapy appears promising, with the current regimen it induced high toxicity rates; therefore, it needs further investigation to preserve efficacy but reduce toxicity.**

The outcome of patients with stage III melanoma is heterogeneous, with a 5-year survival rate of 78, 59, and 40% for patients with stage IIIA, IIIB, and IIIC melanoma, respectively<sup>5</sup>. Patients with macroscopic (including palpable) lymph node metastasis have the poorest outcome with a 2- and 5-year overall survival of approximately 60 and 30%, respectively<sup>6</sup>. Adjuvant radiotherapy after lymph node dissection improves local control, but has no impact on relapse-free survival (RFS) or overall survival<sup>7</sup>. Adjuvant checkpoint inhibition with ipilimumab, a human immunoglobulin G1 (IgG1) monoclonal antibody against cytotoxic T-lymphocyte protein 4 (CTLA-4), and nivolumab, a human IgG4 monoclonal antibody against programmed cell death protein 1 (PD-1), have both been shown to improve RFS in high-risk melanoma<sup>2,8</sup>. Overall survival benefit has been shown for adjuvant ipilimumab<sup>1</sup>, as well as for adjuvant serine/threonine-protein kinase

B-raf (BRAF) + mitogen-activated protein kinase (MEK) inhibition<sup>9</sup>, including for patients with macroscopic metastases. In late-stage melanoma, the combination of ipilimumab + nivolumab achieved superior response rates, progression-free survival, and overall survival compared to monotherapy with ipilimumab (significantly) or nivolumab (numerically)<sup>3,10</sup>. This benefit comes at a cost of a higher grade 3/4 adverse event rate of 59% for ipilimumab + nivolumab, versus 21% for nivolumab and 28% for ipilimumab, respectively<sup>3</sup>. To reduce the toxicity of the ipilimumab + nivolumab combination, an alternative scheme of ipilimumab 1 mg kg<sup>-1</sup> + nivolumab 3 mg kg<sup>-1</sup> (CheckMate 511 trial, NCT02714218) is currently tested in a randomized study. A prior single-arm trial evaluating the combination of standard-dose anti-PD-1 (in this case pembrolizumab) plus reduced-dose ipilimumab provides evidence for reduced toxicity with preserved efficacy<sup>11</sup>.

Neoadjuvant therapy can bear several advantages, allowing one to: (i) determine therapy efficacy within the individual patient for possible additional adjuvant therapy, if needed; (ii) reduce tumor burden before surgery; and (iii) use pathological response data as surrogate outcome markers for relapse-free and overall survival. For these reasons, neoadjuvant therapy has become a standard of care in high tumor burden breast cancer<sup>12</sup>.

In the case of T cell checkpoint blockade, neoadjuvant therapies could bear a fourth, and potentially significant, advantage. T cell checkpoint-blocking antibodies enhance T cell activation the moment an antigen is encountered. Drug exposure during the time the major tumor mass is still present may therefore potentially induce a stronger and broader tumor-specific T cell response. Indeed, recent preclinical data provide support for the superior activity of T cell checkpoint blockade when given before surgery<sup>4</sup>. However, a major challenge for neoadjuvant immunotherapy might be the clinical deterioration of nonresponders, and the onset of severe immune-related adverse events, possibly interfering with potentially curative surgery. Two feasibility trials testing neoadjuvant checkpoint inhibition in high-risk stage III melanoma (NCT02519322 and NCT02437279) were set up to provide an insight into these issues.

<sup>1</sup>Medical Oncology Department, Netherlands Cancer Institute, Amsterdam, The Netherlands. <sup>2</sup>Division of Molecular Oncology & Immunology, Netherlands Cancer Institute, Amsterdam, The Netherlands. <sup>3</sup>Department of Biometrics, Netherlands Cancer Institute, Amsterdam, The Netherlands. <sup>4</sup>Department of Pathology, Netherlands Cancer Institute, Amsterdam, The Netherlands. <sup>5</sup>Surgical Oncology Department, Netherlands Cancer Institute, Amsterdam, The Netherlands. <sup>6</sup>Department of Radiology, Netherlands Cancer Institute, Amsterdam, The Netherlands. <sup>7</sup>Adaptive Biotechnologies, Seattle, WA, USA. <sup>8</sup>NanoString Technologies, Inc., Seattle, WA, USA. \*e-mail: [c.blank@nki.nl](mailto:c.blank@nki.nl); [t.schumacher@nki.nl](mailto:t.schumacher@nki.nl)

Here, we report results from the OpACIN trial (NCT02437279), a randomized phase 1b trial, in high-risk stage III melanoma patients (with palpable disease), testing the feasibility of neoadjuvant ipilimumab + nivolumab, and comparing neoadjuvant versus adjuvant therapy for its capacity to expand tumor-resident T cell clones.

Between August 2015 and October 2016, 20 patients with palpable stage III melanoma were included into the OpACIN trial and randomized to receive either four courses of ipilimumab 3 mg kg<sup>-1</sup> + nivolumab 1 mg kg<sup>-1</sup> every 3 weeks starting at week 6 post-complete regional lymph node dissection (CLND) (adjuvant arm), or to receive two courses ipilimumab 3 mg kg<sup>-1</sup> + nivolumab 1 mg kg<sup>-1</sup> every 3 weeks pre-surgery, followed by CLND at week 6 and another two courses ipilimumab + nivolumab starting at week 12 (thus 6 weeks post-CLND; neoadjuvant arm) (Supplementary Fig. 1). Follow-up was according to the institutional standard for high-risk stage III melanoma, with clinical examination and laboratory testing every 3 months and analysis by computed tomography (CT) scan every 6 months.

At the clinical data cutoff of 9 February 2018, the median follow-up was 25.6 months with a minimum follow-up of 15.9 months for patients that were alive. The demographic and other baseline characteristics of the patients were similar in the two groups (Table 1 and Supplementary Table 1). All patients had a normal lactate dehydrogenase level, normal absolute lymphocyte count, and only two patients in the adjuvant arm had minimally increased C-reactive protein levels. All these markers have been associated with impaired outcome on checkpoint inhibition when elevated<sup>13</sup>. Eight patients had undergone a sentinel node procedure (0/2 tumor-positive in the adjuvant arm, 3/6 tumor-positive in the neoadjuvant arm); none of these patients underwent a subsequent CLND or had received systemic adjuvant therapy before being included in the trial. Tumor programmed cell death ligand 1 (PD-L1) expression  $\geq 1\%$  was found in 40% of patients in the adjuvant arm and 60% of patients in the neoadjuvant arm.

All patients in the neoadjuvant treatment arm underwent CLND at the preplanned surgery time point, no suspected unexpected serious adverse reactions were observed, and none of the surgery-related adverse events were attributed to the study treatment (Table 2). However, only 1/10 patients within each arm received all four courses of ipilimumab + nivolumab. Two patients in the neoadjuvant arm received only a single course (all other patients in the neoadjuvant arm received two courses before surgery), and the median number of courses was two in both arms (adjuvant arm: 1 patient  $\times$  1 course, 5 patients  $\times$  2 courses, 3 patients  $\times$  3 courses, 1 patient  $\times$  4 courses; neoadjuvant arm: 2 patients  $\times$  1 course, 6 patients  $\times$  2 courses, 1 patient  $\times$  3 courses, 1 patient  $\times$  4 courses) (Supplementary Table 1). One patient in the adjuvant arm had to stop treatment due to progression after three cycles. All other patients stopped checkpoint inhibitor therapy due to grade 3/4 adverse events, except for one patient in the neoadjuvant arm who wished to stop due to grade 2 dermatitis (Supplementary Fig. 2).

Treatment-related grade 1/2 adverse events were observed in all patients; grade 3/4 adverse events were observed in 9/10 patients of each arm (Table 2). No previously undescribed adverse events from ipilimumab + nivolumab treatment were observed<sup>3,14</sup>.

Four patients (two in the adjuvant arm and two in the neoadjuvant arm) developed clinically severe treatment-related adverse events: Steven-Johnson syndrome (onset after three cycles); severe colitis (onset after two cycles) requiring four lines of immune suppressive therapy and 10 weeks to recover to grade 1; polyradiculitis (onset after two cycles) requiring three lines of immune suppression and 12 months of rehabilitation to fully recover; and diabetes type 1 (onset after two cycles). Three of these four patients are still free of relapse.

**Table 1 | Clinical baseline characteristics of patients included in the study**

Characteristic	Adjuvant (n=10)	Neoadjuvant (n=10)
Median age, years (range)	54 (40-58)	54 (38-73)
Sex, n (%)		
Men	7 (70)	6 (60)
Women	3 (30)	4 (40)
WHO, n (%)		
0	9 (90)	10 (100)
1	1 (10)	-
AJCC clinical stage		
IIIB	7 (70)	7 (70)
IIIC	3 (30)	3 (30)
Sum of diameter target lesions in mm		
Median (interquartile range)	27 (23-29)	24 (21-31)
Mutation status, n (%)		
<i>BRAF</i> V600 mutant	8 (80)	6 (60)
<i>NRAS</i> mutant	0 (0)	4 (40)
<i>cKIT</i> mutant	0 (0)	0 (0)
<i>BRAF</i> V600/ <i>NRAS</i> / <i>cKIT</i> wildtype	2 (20)	0 (0)
Pretreatment		
Sentinel node procedure	2 (20)	6 (60)
Lymph node dissection	0 (0)	0 (0)
Systemic therapy	0 (0)	0 (0)
LDH < ULN, n (%)	10 (100)	10 (100)
ALC < ULN, n (%)	10 (100)	10 (100)
CRP < ULN, n (%)	8 (80)	10 (100)
Maximum diameter of target lesions,		
Median (range)	27 (11-30)	24 (9-58)
Missing	1	1
PD-L1 expression on tumor cells, n (%)		
<1%	5 (50)	3 (30)
1-50%	2 (20)	4 (40)
>50%	2 (20)	2 (20)
Unknown	1 (10)	1 (10)

PD-L1 immunohistochemistry staining was performed with the 28-8 clone on a Dako platform. AJCC, American Joint Committee on Cancer; ULN, upper limit of normal; ALC, absolute lymphocyte count; CRP, C-reactive protein.

All other adverse events recovered to grade 1. In total, eight patients still require hormonal replacement therapy because of thyroid ( $n=7$ ) or adrenal dysfunction ( $n=5$ ).

In the neoadjuvant arm, 9/10 patients could be evaluated for pathological response; 7/9 (78%) patients achieved profound pathological responses, with 3 pathological complete responses (pCRs), 3 near pCR ( $\leq 10\%$  viable tumor cells), and 1 patient achieving a pathological partial response (pPR  $\leq 50\%$  viable tumor cells). In the patient who could not be evaluated, the revising pathologist observed only one viable micrometastasis of 0.4 mm in the surgical specimen and no signs of necrosis and fibrosis. The initial lesion in the pretreatment biopsy measured at least 3 mm and was not retrieved from the surgical material. For this reason, this patient was defined as nonevaluable.

**Table 2 | Treatment-related adverse events**

Adverse event	All patients (n = 20)		Adjuvant (n = 10)		Neoadjuvant (n = 10)	
	All gradesn (%)	Grade 3/4n (%)	All gradesn (%)	Grade 3/4n (%)	All gradesn (%)	Grade 3/4n (%)
Immunotherapy-related adverse events						
Any adverse event	20 (100)	18 (90)	10 (100)	9 (90)	10 (100)	9 (90)
Elevated ALT	17 (85)	5 (25)	8 (80)	3 (30)	9 (90)	2 (20)
Elevated AST	14 (70)	4 (40)	5 (50)	2 (20)	9 (90)	2 (20)
Diarrhea	12 (60)	6 (30)	6 (60)	2 (20)	6 (60)	4 (40)
Increased GGT	11 (55)	3 (15)	4 (40)	1 (10)	7 (70)	2 (20)
Elevated lipase	11 (55)	8 (40)	5 (50)	5 (50)	6 (60)	3 (30)
Fatigue	10 (50)	-	6 (60)	-	4 (40)	-
Rash	10 (50)	5 (25)	4 (40)	2 (20)	6 (60)	3 (30)
Nausea	9 (45)	-	4 (40)	-	5 (50)	-
Hypothyroidism	8 (40)	-	3 (30)	-	5 (50)	-
Elevated serum amylase	8 (40)	4 (20)	4 (40)	2 (20)	4 (40)	2 (20)
Colitis	7 (35)	6 (30)	4 (40)	3 (30)	3 (30)	3 (30)
Hyperthyroidism	7 (35)	1 (5)	2 (20)	-	5 (50)	1 (10)
Headache	6 (30)	2 (10)	4 (40)	2 (20)	2 (20)	-
Vomiting	6 (30)	3 (15)	3 (30)	1 (10)	3 (30)	2 (20)
Adrenal insufficiency	5 (25)	1 (5)	2 (20)	-	3 (30)	1 (10)
Fever	5 (25)	4 (20)	3 (30)	3 (30)	2 (20)	1 (10)
Pruritus	5 (25)	-	4 (40)	-	1 (10)	-
Abdominal pain	4 (20)	-	3 (30)	-	1 (10)	-
Increased alkaline phosphatase	4 (20)	-	2 (20)	-	2 (20)	-
Flu-like symptoms	4 (20)	1 (5)	4 (40)	1 (10)	-	-
Anemia	3 (15)	-	2 (20)	-	1 (10)	-
Cough	3 (15)	-	2 (20)	-	1 (10)	-
Hypophosphatemia	3 (15)	3 (15)	1 (10)	1 (10)	2 (20)	2 (20)
Weight loss	3 (15)	-	1 (10)	-	2 (20)	-
Hypokalemia	2 (10)	1 (5)	-	-	2 (20)	1 (10)
Hyponatremia	2 (10)	2 (10)	-	-	2 (20)	2 (20)
Hypophysitis	2 (10)	2 (10)	2 (20)	2 (20)	-	-
Increased blood bilirubin	1 (5)	1 (5)	-	-	1 (10)	1 (10)
Cerebral demyelination	1 (5)	1 (5)	1 (10)	1 (10)	-	-
Diabetic ketoacidosis	1 (5)	1 (5)	-	-	1 (10)	1 (10)
Dizziness	1 (5)	1 (5)	-	-	1 (10)	1 (10)
Hyperglycemia	1 (5)	1 (5)	-	-	1 (10)	1 (10)
Glucose intolerance	1 (5)	1 (5)	-	-	1 (10)	1 (10)
Meningoradiculitis	1 (5)	1 (5)	1 (10)	1 (10)	-	-
Surgery-related adverse events						
Any	18 (90)	3 (15)	9 (90)	2 (20)	9 (90)	1 (10)
Seroma	18 (90)	-	9 (90)	-	9 (90)	-
Wound infection	8 (40)	3 (15)	4 (40)	2 (20)	4 (40)	1 (10)
Limb edema	3 (15)	-	1 (10)	-	2 (20)	-
Wound dehiscence	3 (15)	-	2 (20)	-	1 (10)	-

Treatment-related events of all grades are reported when occurring in more than two patients. ALT, Alanine aminotransferase; AST, aspartate aminotransferase; GGT, gamma-glutamyl transferase.

Interestingly, the CT evaluation according to RECIST guidelines (version 1.1) underestimated these pathological responses, and the responses did not correlate with mutational burden (Fig. 1a and Supplementary Fig. 3). None of the patients who achieved a pathological response within the neoadjuvant arm has relapsed thus far (median follow-up of 21.6 months after surgery with a minimum

of 15.9 months), making pathological response, which is thus far not an established response evaluation marker, a promising marker for neoadjuvant immunotherapy evaluation. In line with these data, a recently published trial testing neoadjuvant nivolumab in non-small-cell lung cancer also found that radiological response underestimated pathological response<sup>15</sup>.

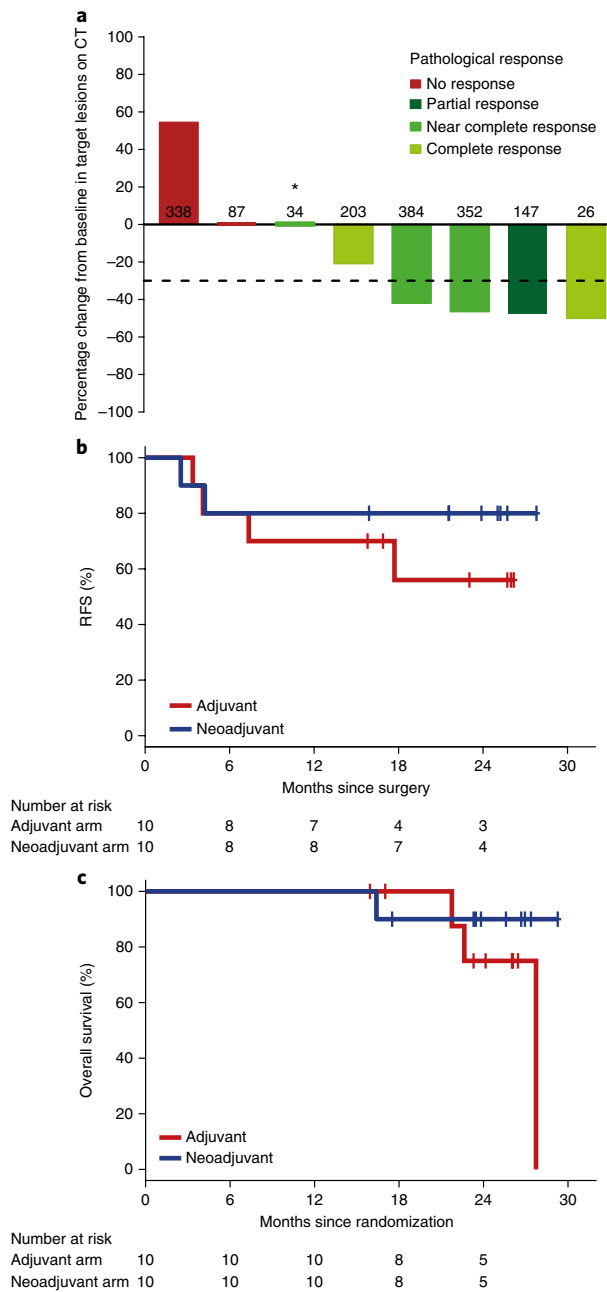


**Fig. 1 | Waterfall plot, RFS, and overall survival.** **a**, Radiological response of patients receiving neoadjuvant therapy as assessed by a radiologist (two patients missing due to missing presurgery CT scan). The waterfall plot shows the objective response measured as the change from baseline in the sum of the shortest diameters of all target lesions. The bar colors reflect the pathological response (red: no response; dark green: partial response; middle-shade green: near-complete response; light green: complete response). The number above or in the bar represents the total number of non-synonymous and frameshift mutations per tumor, as identified by whole-exome sequencing of pretreatment biopsies. \*This patient had a palpable, positron emission tomography-positive, histologically proven, tumor-positive lymph node, which was <10 mm at the short axis before start of treatment and was still <10 mm on the CT scan performed at week 6. **b**, Kaplan–Meier estimate of RFS. In the adjuvant arm, distant metastases were reported for four patients. In the neoadjuvant arm, local recurrence was reported for one patient and distant metastasis also for one patient. **c**, Kaplan–Meier estimate of overall survival. In the adjuvant arm, death was reported for four patients. In the neoadjuvant arm, death was reported for one patient.

At data cutoff, two patients in the neoadjuvant arm (the two nonresponding patients), and four patients in the adjuvant arm have relapsed (Fig. 1b). One patient in each arm developed a lymph node–only relapse and underwent a second lymph node dissection. Distant metastases requiring systemic therapy were observed in one patient in the neoadjuvant arm and in three patients in the adjuvant arm. All four patients had a *BRAF*<sup>V600E/K</sup> mutation–positive tumor and received BRAF+MEK inhibition among other therapies, but died because of disease progression (Fig. 1c). In the neoadjuvant arm, one patient died after 12 months of systemic treatment with dabrafenib+trametinib. In the adjuvant arm, the first patient died after 15 months of systemic treatment with dabrafenib+trametinib, followed by pembrolizumab and palliative radiotherapy. The second patient died after 24 months, having received 6 months of treatment with dabrafenib+trametinib, followed by palliative resection, palliative radiotherapy, and tumor-infiltrating lymphocyte therapy. The third patient died after 16 months of treatment with dabrafenib+trametinib and palliative radiotherapy.

The second co-primary endpoint of this trial was to compare neoadjuvant versus adjuvant ipilimumab+nivolumab for their capacity to expand circulating tumor-specific T cells by means of major histocompatibility complex (MHC) multimer staining of tumor neoantigen-specific T cells in peripheral blood<sup>16</sup>. In contrast to the frequent detection of neoantigen-specific T cell responses in the peripheral blood of patients with stage IV melanoma, we detected only a single neoantigen-specific T cell response in the peripheral blood of two of the first eight patients analyzed, making this technique unfeasible for the planned descriptive comparison (Supplementary Fig. 4).

Additionally, we analyzed tumor material from 18/20 patients by T cell receptor (TCR) sequencing (immunoSEQ Assay; Adaptive Biotechnologies) to identify T cell clones that were most prevalent at the tumor site and to describe their presence and expansion in peripheral blood during ipilimumab+nivolumab treatment.

Analysis of the entire TCR repertoire in baseline tumor samples revealed that a reduced T cell tumor infiltrate (estimated by TCR gene rearrangements per diploid genome) and a lower productive T cell clonality (more diverse tumor-infiltrating lymphocyte repertoire) within the tumor (Supplementary Fig. 5a, toward the lower left quadrant) was regularly found in patients who relapsed after ipilimumab+nivolumab.

Subsequently, the top 100 tumor-resident T cell clones were tracked in the peripheral blood of each patient and analyzed for expansion between the start and week 6 of checkpoint inhibition (Fig. 2a–e). We found neoadjuvant ipilimumab+nivolumab to expand more tumor-resident T cell clones in the peripheral blood compared to adjuvant ipilimumab+nivolumab (Fig. 2a). This was the case for tumor-resident T cell clones that were already detectable at baseline in peripheral blood (present at baseline) (Fig. 2b), as well as for tumor-resident clones that were below the limit of detection at baseline in peripheral blood but became detectable after therapy (newly detected) (Fig. 2c). When comparing patients who relapsed with relapse-free patients, we found that all patients who relapsed displayed lower numbers of newly detected T cell clones, while no difference in expansion of T cell clones present at baseline was observed (Fig. 2d,e). Analysis of significantly expanded T cell clones in peripheral blood (differential abundance), instead of the top 100 tumor-resident clones, revealed the same pattern (Supplementary Fig. 5b,c), with again a more profound expansion observed in patients in the neoadjuvant arm. The extent of expansion per clone (as measured by the fold expansion of each tumor-resident clone) was also higher in the neoadjuvant arm (Supplementary Fig. 6a,b).

Parallel analysis of 29 immune parameters (Supplementary Table 2) by NanoString spatial microscopy (Supplementary Fig. 7a–c) on baseline tumor biopsies revealed that low CD3,  $\beta_2$  microglobulin

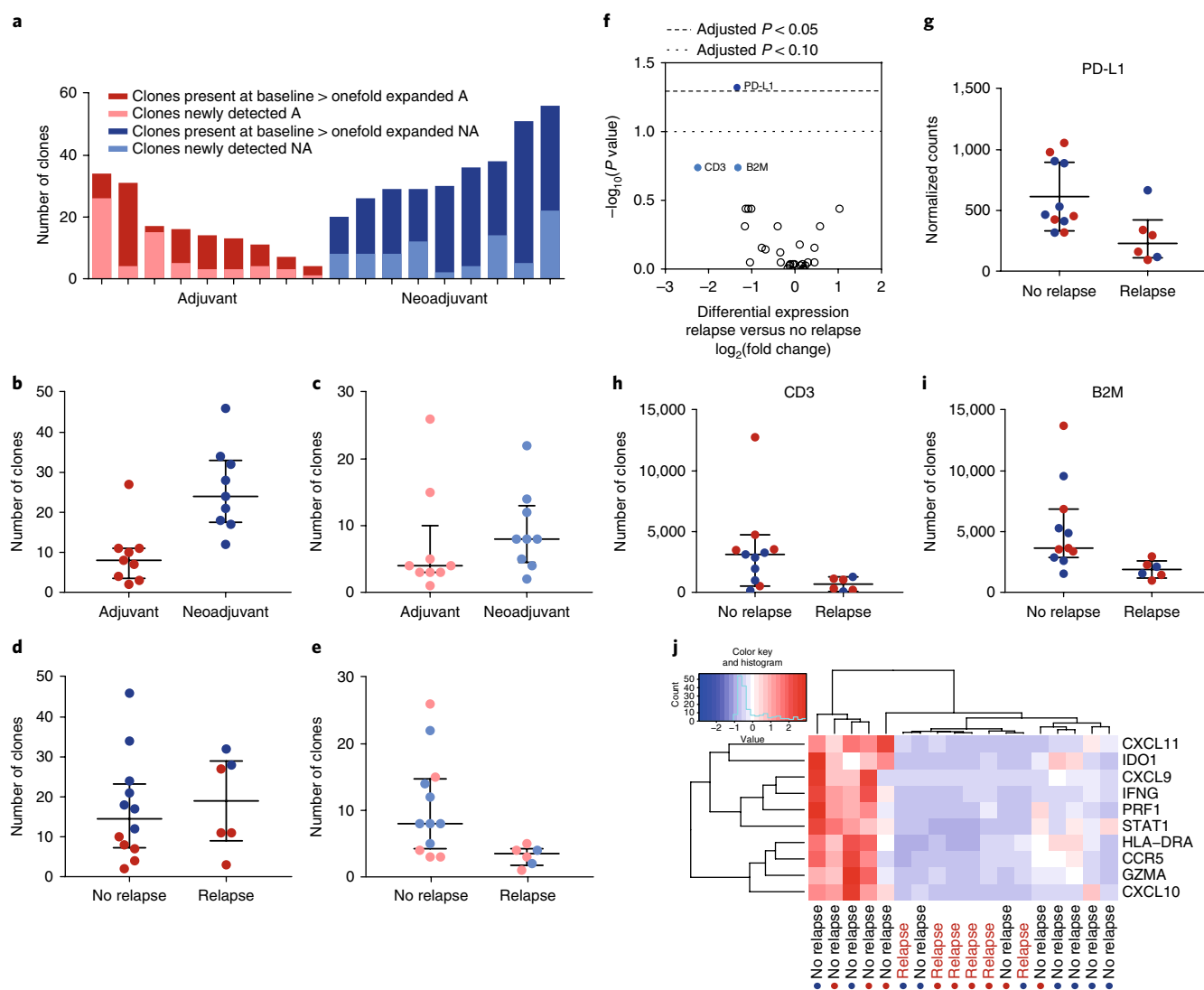


**Fig. 2 | TCR sequencing, DSP, and RNA sequencing.** **a–e**, TCR sequencing. TCR repertoires were characterized for preimmunotherapy tumor samples using the ImmunoSEQ Assay, resulting in the identification of 196–13,196 productive rearrangements identified per patient. The top 100 TCR sequences (tumor-resident clones) were analyzed for presence in peripheral blood of the patients at baseline and at week 6. **a**, Number of top 100 tumor-resident clones that were present in peripheral blood at baseline and expanding and/or newly detected are shown for each patient for the neoadjuvant (NA) and adjuvant (A) arm. **b**, The number of top 100 tumor-resident clones that expanded >1-fold during treatment per treatment arm. **c**, The number of top 100 tumor-resident clones that were not detectable at baseline in peripheral blood but became detectable after treatment per treatment arm. **d**, The number of top 100 tumor-resident clones detected at baseline and expanded >1-fold at week 6 according to relapse status. **e**, The number of clones not detectable at baseline but detected at week 6 (newly detected clones), according to relapse status. In **b–e**, The median and interquartile range are shown,  $n=18$  patients (9 adjuvant, 9 neoadjuvant; 12 without relapse, 6 with relapse). Every dot represents one patient, and the color indicates the treatment arm: adjuvant (red); neoadjuvant (blue). **f–i**, DSP analysis of pretreatment tumor biopsies. The S100 B visualization marker was used to identify tumor-rich ROIs. Protein profiling of ROIs was achieved using an oligo-conjugated antibody panel and read out with NanoString barcodes. **f**, Volcano plot showing differential expression of proteins between patients with and without relapse. Proteins associated with adaptive immunity, including PD-L1, have decreased expression in patients with a subsequent relapse. The horizontal position shows the magnitude of a protein's association with relapse status; the vertical position shows the  $-\log_{10}(P \text{ value})$ , which increases with statistical significance. The dotted lines represent the adjusted  $P$  value cutoffs. Comparisons were analyzed using a two-tailed Student's  $t$ -test,  $n=17$  patients (11 without relapse and 6 with relapse). **g–i**, Patients with relapse have lower pretreatment B2M, lower PD-L1, and lower CD3 protein expression in tumor-enriched ROIs. The median and interquartile range are shown,  $n=17$  patients (11 without relapse and 6 with a relapse). **j**, RNA sequencing. Hierarchical clustering of IFN- $\gamma$  signature including ten genes developed for predicting the response of patients with melanoma on anti-PD1 treatment<sup>18</sup>. Gene-level expression values were computed as transcripts per million and were normalized to Z-scores before clustering. Positive values (red) indicate higher expression and negative values (blue) indicate lower expression. Every column represents one patient for whom clinical outcome is depicted; the colored dots below the clinical outcome indicate the treatment arm: adjuvant (red); neoadjuvant (blue).

(B2M) and PD-L1 molecule expression (the latter both known to be upregulated on exposure to interferon- $\gamma$  (IFN- $\gamma$ )<sup>17</sup>) within the tumor areas was strongly associated with relapse after neoadjuvant or adjuvant ipilimumab + nivolumab (Fig. 2f–i). Similarly, low RNA expression of the IFN- $\gamma$  signature<sup>18</sup> was associated with relapse after

ipilimumab + nivolumab, independent of neoadjuvant or adjuvant treatment (Fig. 2j). In contrast, none of the patients with a high or intermediate IFN- $\gamma$  signature has relapsed so far. We found that 4/5 patients with human leukocyte antigen class I allele loss had a high or intermediate IFN- $\gamma$  signature in the pretreatment tumor

biopsy (Supplementary Fig. 8 a,b), suggestive of preexisting CD8<sup>+</sup> T cell pressure. The remaining patient with a low IFN- $\gamma$  signature had a pPR and has not relapsed to date. Translational research data for every patient are displayed in Supplementary Table 1 and Supplementary Fig. 8b (IFN- $\gamma$  signature).

OpACIN is the first trial testing the feasibility of neoadjuvant versus adjuvant ipilimumab 3 mg kg<sup>-1</sup> + nivolumab 1 mg kg<sup>-1</sup> in stage III melanoma. Both adjuvant single-agent ipilimumab and nivolumab have been shown to improve the outcome of stage 3 melanoma, with nivolumab achieving a significantly higher relapse-free rate compared to ipilimumab<sup>1,2</sup>; hence, our rationale to test their combination in stage III melanoma.

Ipilimumab + nivolumab treatment in stage III melanoma was feasible in our trial. All patients in the neoadjuvant arm underwent CLND at the preplanned time point, and no surgery-related adverse events were attributed to the prior immunotherapy. However, in both arms grade 3/4 toxicity was highly prevalent and more frequent than would be predicted from data in stage IV melanoma (90% in both the adjuvant and neoadjuvant arm versus 59% in late-stage disease)<sup>3</sup>, resulting in early treatment discontinuation in 18/20 patients. In two other trials (to date, only presented) that have tested ipilimumab + nivolumab in stage III melanoma, similar high toxicity rates have been observed (73 and 90% grade 3/4 toxicity, respectively)<sup>19,20</sup>. These observed high toxicity rates make the current standard dosing of ipilimumab + nivolumab unfeasible for broad application in the neoadjuvant or adjuvant setting.

At the same time, tumor response rate in the neoadjuvant arm was high, with 7/9 evaluable patients achieving profound pathological responses after only two courses of therapy. Therefore, neoadjuvant treatment in stage III melanoma may lead to surgical de-escalation with less extensive procedures, similar to the situation in breast cancer<sup>21</sup>.

The combination of high pathological response rates and high toxicity suggests that patients with earlier-stage disease may have a lower degree of systemic immune suppression<sup>22</sup>. For this reason, a less intense treatment schedule, with a reduced number of courses and/or dose adjustment of ipilimumab, may potentially be sufficient in early-stage melanoma to obtain a similar efficacy. This hypothesis is currently being tested in a subsequent trial (OpACIN-neo, NCT02977052), with the aim to preserve efficacy while reducing toxicity. In stage IV disease these alternative schemes have been analyzed retrospectively and in a single-arm trial, indicating reduced toxicity but preserved efficacy<sup>11,23</sup>.

At data lock (median follow-up of 25.6 months) none of the responders within the neoadjuvant cohort has relapsed, making pathological response a promising early marker for outcome in future neoadjuvant combination trials. In addition, response assessment at the time of surgery allows switching locally progressing patients to other therapeutic regimens, such as adjuvant BRAF + MEK inhibition in case of *BRAF*<sup>V600E/K</sup>-mutant disease<sup>9</sup>, or the provision of additional nivolumab consolidation therapy following adjuvant radiotherapy in *BRAF* wild-type patients.

Two patients relapsed in the neoadjuvant arm and four in the adjuvant arm. These observed RFS data are already relatively mature, as 80% of all relapses in resected stage III melanoma occur within the first 2 years post-CLND<sup>24</sup>. The high 2-year RFS rate observed in the neoadjuvant arm (8/10, 80%) is also in line with data from another trial testing adjuvant ipilimumab + nivolumab in stage III melanoma (78% RFS at 2 years)<sup>20</sup>. (Neo)adjuvant ipilimumab + nivolumab seems to be superior to adjuvant ipilimumab in macroscopic (palpable) stage III disease (42% RFS at 18 months follow-up)<sup>24</sup>, as well as potentially to adjuvant nivolumab (66.4% RFS at 18 months follow-up)<sup>2</sup>. However, adjuvant nivolumab showed a clearly favorable toxicity profile<sup>2</sup>, indicating the need for trials that aim to identify more feasible combination schedules of ipilimumab + nivolumab for patients with stage III disease.

Preclinical data argue for improved efficacy of neoadjuvant compared to adjuvant checkpoint inhibition in eradicating metastatic disease<sup>4</sup>. While this trial was not powered to draw such conclusions based on clinical data, analysis of the expansion of tumor-resident T cell clones in peripheral blood demonstrates a significant difference favoring neoadjuvant treatment. Specifically, expansion of T cell clones that were detected at baseline as well as newly detected T cell clones was superior in neoadjuvant-treated patients. Of note, all patients who have relapsed so far showed inferior expansion of newly detected T cell clones on therapy. In a preclinical model, PD-1 blockade enhanced survival of subdominant T cell clones, thereby leading to epitope spreading in the tumor-specific CD8<sup>+</sup> T cell response<sup>25</sup>. In addition, broadening of tumor-specific T cell response in peripheral blood was also observed in stage IV patients treated with ipilimumab<sup>26</sup>. Whether the observed expansion of newly detected peripheral blood T cell clones represents such epitope spreading warrants further investigation. Compared to prior data in stage IV melanoma, T cell responses against defined neoantigens were observed in only a small fraction of patients. Conceivably, prolonged exposure of the immune system to tumor cells may lead to the more frequent detection of neoantigen-specific T cell reactivity in stage IV disease, a model that remains to be tested in a side-by-side comparison.

In line with observations from PD-1 or PD-1 + CTLA-4 blockade in late-stage melanoma<sup>3,27,28</sup>, low tumor T cell infiltration (as measured by CD3), lower MHC expression (as measured by B2M), and low PD-L1 expression were associated with relapse after (neo) adjuvant ipilimumab + nivolumab. In addition, similar to the data from patients treated with anti-PD-1 in stage IV disease<sup>18</sup>, we observed that a high or intermediate IFN- $\gamma$  RNA signature was a reliable predictor for the clinical outcome of the patients; this needs to be confirmed in a larger cohort of patients treated with neoadjuvant ipilimumab + nivolumab.

In summary, OpACIN is the first trial comparing neoadjuvant with adjuvant immune checkpoint combination therapy, demonstrating a high clinical activity of neoadjuvant therapy, and possible superiority of neoadjuvant treatment, as based on immunomonitoring. Toxicity was higher than expected, arguing for the development of reduced intensity regimens in this disease setting. The expansion of tumor-resident T cell clones and favorable IFN- $\gamma$  signatures may also serve as biomarkers in other neoadjuvant immunotherapy trials. In that way, OpACIN can serve as a template for other neoadjuvant combination trials in melanoma and beyond.

**URLs.** STAR RNA-seq aligner, <https://github.com/alexdobin/STAR>; Salmon, <https://combine-lab.github.io/salmon>; Burrows–Wheeler Aligner, <http://bio-bwa.sourceforge.net/>; IndelRealigner, [https://software.broadinstitute.org/gatk/documentation/tooldocs/3.8-0/org\\_broadinstitute\\_gatk\\_tools\\_walkers\\_indels\\_IndelRealigner.php](https://software.broadinstitute.org/gatk/documentation/tooldocs/3.8-0/org_broadinstitute_gatk_tools_walkers_indels_IndelRealigner.php); BaseRecalibrator, [https://software.broadinstitute.org/gatk/documentation/tooldocs/3.8-0/org\\_broadinstitute\\_gatk\\_tools\\_walkers\\_bqsr\\_BaseRecalibrator.php](https://software.broadinstitute.org/gatk/documentation/tooldocs/3.8-0/org_broadinstitute_gatk_tools_walkers_bqsr_BaseRecalibrator.php); SomaticSniper, <https://github.com/genome/somatic-sniper>; IndelGenotyper, <https://gatkforums.broadinstitute.org/gatk/discussion/5272/indelgenotyper>.

### Online content

Any methods, additional references, Nature Research reporting summaries, source data, statements of data availability and associated accession codes are available at <https://doi.org/10.1038/s41591-018-0198-0>.

Received: 13 April 2018; Accepted: 6 August 2018;

Published online: 8 October 2018

### References

1. Eggermont, A. M. et al. Prolonged survival in stage III melanoma with ipilimumab adjuvant therapy. *N. Engl. J. Med.* **375**, 1845–1185 (2016).

2. Weber, J. et al. Adjuvant nivolumab versus ipilimumab in resected stage III or IV melanoma. *N. Engl. J. Med.* **377**, 1824–1835 (2017).
3. Wolchok, J. D. et al. Overall survival with combined nivolumab and ipilimumab in advanced melanoma. *N. Engl. J. Med.* **377**, 1345–1356 (2017).
4. Liu, J. et al. Improved efficacy of neoadjuvant compared to adjuvant immunotherapy to eradicate metastatic disease. *Cancer Discov.* **6**, 1382–1399 (2016).
5. Balch, C. M. et al. Final version of 2009 AJCC melanoma staging and classification. *J. Clin. Oncol.* **27**, 6199–6206 (2009).
6. Balch, C. M. et al. Prognostic factors analysis of 17,600 melanoma patients: validation of the American Joint Committee on Cancer melanoma staging system. *J. Clin. Oncol.* **19**, 3622–3634 (2001).
7. Burmeister, B. H. et al. Adjuvant radiotherapy versus observation alone for patients at risk of lymph-node field relapse after therapeutic lymphadenectomy for melanoma: a randomised trial. *Lancet Oncol.* **13**, 589–597 (2012).
8. Eggermont, A. M. et al. Adjuvant ipilimumab versus placebo after complete resection of high-risk stage III melanoma (EORTC 18071): a randomised, double-blind, phase 3 trial. *Lancet Oncol.* **16**, 522–530 (2015).
9. Long, G. V. et al. Adjuvant dabrafenib plus trametinib in stage III BRAF-mutated melanoma. *N. Engl. J. Med.* **377**, 1813–1823 (2017).
10. Larkin, J. et al. Combined nivolumab and ipilimumab or monotherapy in untreated melanoma. *N. Engl. J. Med.* **373**, 1270–1271 (2015).
11. Long, G. V. et al. Standard-dose pembrolizumab in combination with reduced-dose ipilimumab for patients with advanced melanoma (KEYNOTE-029): an open-label, phase 1b trial. *Lancet Oncol.* **18**, 1202–1210 (2017).
12. Steenbruggen, T. G. et al. Neoadjuvant therapy for breast cancer: established concepts and emerging strategies. *Drugs* **77**, 1313–1336 (2017).
13. Blank, C. U., Haanen, J. B., Ribas, A. & Schumacher, T. N. CANCER IMMUNOLOGY. The “cancer immunogram”. *Science* **352**, 658–660 (2016).
14. Larkin, J. et al. Neurologic serious adverse events associated with nivolumab plus ipilimumab or nivolumab alone in advanced melanoma, including a case series of encephalitis. *Oncologist* **22**, 709–718 (2017).
15. Forde, P. M. et al. Neoadjuvant PD-1 blockade in resectable lung cancer. *N. Engl. J. Med.* **378**, 1976–1986 (2018).
16. van Rooij, N. et al. Tumor exome analysis reveals neoantigen-specific T-cell reactivity in an ipilimumab-responsive melanoma. *J. Clin. Oncol.* **31**, e439–442 (2013).
17. Blank, C. et al. PD-L1/B7H-1 inhibits the effector phase of tumor rejection by T cell receptor (TCR) transgenic CD8<sup>+</sup> T cells. *Cancer Res.* **64**, 1140–1145 (2004).
18. Ayers, M. et al. IFN- $\gamma$ -related mRNA profile predicts clinical response to PD-1 blockade. *J. Clin. Invest.* **127**, 2930–2940 (2017).
19. Reddy, S. M. et al. Neoadjuvant nivolumab versus combination ipilimumab and nivolumab followed by adjuvant nivolumab in patients with resectable stage III and oligometastatic stage IV melanoma: preliminary findings. In *32nd SITC Annual Meeting* abstr. O15.(National Harbor, MD, USA, 2017).
20. Eroglu, Z. et al. Mature results of combination nivolumab plus ipilimumab as adjuvant therapy in stage IIIC/IV melanoma. *Annual Meeting Society of Melanoma Research (SMR)* (Brisbane, Queensland, Australia, 2017).
21. Straver, M. E., Loo, C. E., Alderliesten, T., Rutgers, E. J. & Vrancken Peeters, M. T. Marking the axilla with radioactive iodine seeds (MARI procedure) may reduce the need for axillary dissection after neoadjuvant chemotherapy for breast cancer. *Br. J. Surg.* **97**, 1226–1231 (2010).
22. Lui, V. K., Karpuchas, J., Dent, P. B., McCulloch, P. B. & Blajchman, M. A. Cellular immunocompetence in melanoma: effect of extent of disease and immunotherapy. *Br. J. Cancer* **32**, 323–330 (1975).
23. Meerveld-Eggink, A. et al. Short-term CTLA-4 blockade directly followed by PD-1 blockade in advanced melanoma patients: a single-center experience. *Ann. Oncol.* **28**, 862–867 (2017).
24. Eggermont, A. M. et al. Ipilimumab versus placebo after complete resection of stage III melanoma: initial efficacy and safety results from the EORTC 18071 phase III trial. *J. Clin. Oncol.* **32**, LBA9008–LBA9008 (2014).
25. Memarnejadian, A. et al. PD-1 blockade promotes epitope spreading in anticancer CD8<sup>+</sup> T cell responses by preventing fratricidal death of subdominant clones to relieve immunodomination. *J. Immunol.* **199**, 3348–3359 (2017).
26. Kvistborg, P. et al. Anti-CTLA-4 therapy broadens the melanoma-reactive CD8<sup>+</sup> T cell response. *Sci. Transl. Med.* **6**, 254ra128 (2014).
27. Tumeh, P. C. et al. PD-1 blockade induces responses by inhibiting adaptive immune resistance. *Nature* **515**, 568–571 (2014).
28. Zaretsky, J. M. et al. Mutations associated with acquired resistance to PD-1 blockade in melanoma. *N. Engl. J. Med.* **375**, 819–829 (2016).

## Acknowledgements

We thank the patients and their families for participating in the study. We thank A. Gangaev for performing the experiments involving MHC tetramer staining; M. Valenti, T. Kuilman, and other members from the Blank, Peeper, and Schumacher laboratory for valuable discussions; W. Uytendinck, A. Koenen, M. Wouters, and J. vd Hage for the clinical care of the patients included in the trial; C. Bierman for assisting with the pathological revisions of tumor samples; the NKI-AVL flow facility and the NKI-AVL Core Facility Molecular Pathology & Biobanking for supplying the NKI-AVL biobank material and/or laboratory support; E. Hooijberg for supervising the immunohistochemistry analysis; S. Vanhoutin for financial management; A. Cesano for scientific input on the NanoString analyses; and D. Walker, C. Pfeiffer, B. Lamon, B. Stegenga, and V. Goodman from Bristol-Myers Squibb for scientific input and support.

## Author contributions

C.U.B. and T.N.S. designed the study and wrote the manuscript. E.A.R. analyzed and interpreted the clinical and translational data. L.F.F. performed the bioinformatics analyses. K.S. performed the statistical analysis on the clinical data. B.vd.W. assessed the pathological response of neoadjuvant-treated patients. M.vd.B. and D.P. performed the experiments for the MHC tetramer analysis. P.K. supervised the MHC tetramer analysis. C.U.B., J.V.v.T., J.B.A.G.H., H.A.M., S.A., and S.T.M., were responsible for the clinical care of the patients. L.G.G.-O. was responsible for data management. L.M.P. is the clinical project manager for this study. A. Broeks was responsible for storing and processing the tumor samples. A. Bruining performed the radiological evaluations. S.W. was responsible for the DSP analysis. R.M.G. was responsible for TCR sequencing. H.v.T. created the statistical design. A.C.J.v.A. performed the surgeries. A.C.J.v.A., D.S.P., O.K., and J.B.A.G.H. gave critical input. All authors critically revised the manuscript.

## Competing interests

C.U.B. reports personal fees for advisory roles for MSD, BMS, Roche, GSK, Novartis, Pfizer, GenMab, and Lilly, and grants from BMS, NanoString, and Novartis, outside the submitted work. E.A.R. reports travel support from NanoString Technologies and MSD, outside the submitted work. L.F.F., K.S., B.vd.W., P.K., O.K., M.vd.B., D.P., A. Broeks., H.A.M., S.A., S.T.M., L.M.P., L.G.G.-O., A. Bruining, and H.v.T. have nothing to disclose. J.V.v.T. reports travel support from Roche, outside the submitted work. R.M.G. has a financial interest in Adaptive Biotechnologies. S.W. is an employee of and is a stockholder in NanoString Technologies, has an advisory role with Roche, and is a former employee of the Oncofactor Corporation, outside the submitted work. D.S.P. reports research support from BMS. J.B.A.G.H. reports that NKI received fees for his advisory roles from BMS, MSD, Roche, Neon Therapeutics, Immunocore, Novartis, AstraZeneca/MedImmune, Pfizer, and Ipsen; NKI received grants from BMS, Merck, Novartis, and Neon Therapeutics, outside the submitted work. A.C.J.v.A. reports personal fees for an advisory role with Amgen, Bristol-Myers Squibb, Novartis, MSD-Merck, and Merck-Pfizer, and grants from Amgen and Novartis, all outside the submitted work. T.N.S. is consultant for Adaptive Biotechnologies, AIMM Therapeutics, Amgen, Neon Therapeutics, Scenic Biotech, and reports grant/research support from Merck, Bristol-Myers Squibb, and Merck KGaA; he is a stockholder in AIMM Therapeutics and Neon Therapeutics.

## Additional information

**Supplementary information** is available for this paper at <https://doi.org/10.1038/s41591-018-0198-0>.

**Reprints and permissions information** is available at [www.nature.com/reprints](http://www.nature.com/reprints).

**Correspondence and requests for materials** should be addressed to C.U.B. or T.N.S.

**Publisher's note:** Springer Nature remains neutral with regard to jurisdictional claims in published maps and institutional affiliations.

© The Author(s), under exclusive licence to Springer Nature America, Inc. 2018

## Methods

**Patients.** Eligible patients were 18 years of age or older; they had histologically confirmed resectable stage III melanoma with palpable lymph node metastases and no history of in-transit metastases within the last 6 months. A World Health Organization Performance Status of 0 or 1 and normal lactate dehydrogenase levels were required. Exclusion criteria included: autoimmune disease; human immunodeficiency virus or hepatitis B or C infection; prior immunotherapy targeting CTLA-4, PD-1, or PD-L1; immunosuppressive medication within 6 months before study inclusion; and radiotherapy before or after surgery within the trial.

**Trial design and endpoints.** In this randomized phase 1b trial, 20 patients were randomized 1:1 to receive either 4 courses of ipilimumab 3 mg kg<sup>-1</sup> + nivolumab 1 mg kg<sup>-1</sup> every 3 weeks starting at week 6 post-CLND (adjuvant arm), or 2 courses of ipilimumab 3 mg kg<sup>-1</sup> + nivolumab 1 mg kg<sup>-1</sup>, every 3 weeks presurgery, followed by CLND at week 6 and another 2 courses ipilimumab + nivolumab starting at week 12 (thus 6 weeks post-CLND; neoadjuvant arm).

Co-primary endpoints were safety (as measured by the frequency of suspected unexpected serious adverse reactions in both arms) and feasibility (neoadjuvant arm only, as measured by CLND at the preplanned time point), and the comparison of the immune-activating capacity of neoadjuvant versus adjuvant ipilimumab + nivolumab. Immune-activating capacity was initially defined in the protocol as the ability to increase the magnitude and/or breadth of the neoantigen-specific T cell response in the time interval from pre- to post-adjuvant therapy in peripheral blood, using MHC tetramer staining for neoantigen-specific T cells in the peripheral blood<sup>16</sup>.

**Assessments.** Response to neoadjuvant therapy was scored on CT scan by a radiologist according to the RECIST guidelines (version 1.1) and reviewed by one blinded pathologist, who scored the percentage vital tumor cells in the surgery material. The presurgery CT scan was not obtained for two patients in the neoadjuvant arm (the study team missed ordering these CT scans). Starting at week 18, patients in both trial arms were assessed for relapse every 3 months for 3 years by physical examination and laboratory testing. Subsequent structured follow-up was carried out according to the current Dutch melanoma guidelines (year 4 and 5, physical examination and laboratory testing every 6 months; year 6–10, once a year). CT scans of the thorax and abdomen were performed every 6 months according to the Netherlands Cancer Institute (NKI) standard.

RFS was defined as the time from surgery until the date of first relapse (local, regional, or distant metastasis) from any cause. Overall survival was defined as the time from randomization until death from any cause. Data on recurrence and survival were censored at the last date of contact with no evidence of disease.

Data on adverse events were collected for each group using the Common Terminology Criteria for Adverse Events (version 4.03). Resolution of an immune-related adverse event of grade 3 or 4 was defined as an improvement to grade 1 or less.

**Trial oversight.** The protocol and amendments for this trial were reviewed by the independent medical ethics committee of the NKI. The trial was conducted in accordance with the Good Clinical Practice guidelines as defined by the International Conference on Harmonization. All patients provided written informed consent before enrollment. This investigator-initiated trial was designed by the first and last author and funded by Bristol-Myers Squibb through the International Immuno-Oncology Network, with the NKI as the sponsor.

Data were collected by the sponsor and analyzed in collaboration with all authors. No data or safety monitoring committee was created, since the sponsor reported annually to the medical ethics committee.

The first draft of the manuscript was written by the first author; all other authors contributed to subsequent drafts and provided final approval before submission for publication. All authors vouch for the accuracy and completeness of the data and the analyses reported and confirm adherence to the protocol.

**Collection of blood and tumor samples.** Blood samples, including peripheral blood mononuclear cells, were collected at baseline, during treatment, and during follow-up (Supplementary Fig. 1). Pretreatment tumor biopsies were taken from an affected lymph node by a trained radiologist using ultrasound. The obtained samples were immediately snap-frozen and formalin-fixed and paraffin-embedded (FFPE).

**Statistical considerations.** The study treatment scheme was defined to be unsafe and not feasible if 2 out of the first 5 patients (point estimate 0.4, 95% confidence interval 0.05–0.85) or 4 out of the 10 (point estimate 0.4, 95% confidence interval 0.12–0.74) patients in the neoadjuvant arm experienced immune-related adverse events leading to delayed surgery (not performed in week 6) or experienced grade 3/4 suspected unexpected serious adverse reactions after surgery that were attributed to the pre-surgery immunotherapy. Median follow-up was calculated using inverted Kaplan–Meier approach.

Analyses of the alterations of tumor-specific T cell responses and immunohistochemistry analyses were descriptive. Analyses were performed using R (version 3.3.1) and GraphPad Prism (version 7.03; GraphPad Software).

**TCR sequencing.** Immunosequencing of the CDR3 regions of human TCRβ chains was performed on baseline tumor biopsies and peripheral blood mononuclear cells pre- and post-immunotherapy using the ImmunoSEQ Assay. The extracted genomic DNA was amplified in a bias-controlled multiplex PCR, followed by high-throughput sequencing. Sequences were collapsed and filtered to identify and quantitate the absolute abundance of each unique TCRβ CDR3 region for further analysis, as previously described<sup>29–31</sup>.

The 100 most prevalent tumor-resident T cell clones were subsequently analyzed for their presence and frequency in peripheral blood at the start of ipilimumab + nivolumab therapy and after 6 weeks of ipilimumab + nivolumab therapy in both treatment arms. (For a schematic trial overview, see Supplementary Fig. 1.) Analyses were performed for 18 patients; the data for 2 patients (one in each arm) could not be analyzed because there were not enough tumor cells in the frozen biopsy to isolate DNA.

**Digital spatial profiling (DSP).** DSP analysis of 29 immune-related surface antigens (Supplementary Table 1) was performed by NanoString spatial microscopy (for a schematic overview, see Supplementary Fig. 7a) on FFPE pretreatment tumor biopsies. Analyses were performed for 17 patients because the FFPE biopsies from three patients contained insufficient tumor cells to be analyzed. Slides were stained with 29 oligo-conjugated antibodies and S100 calcium-binding protein B and CD45. S100 B was used as a visualization marker to identify tumor-rich regions of interest (ROIs) and CD45 to identify immune-infiltrated ROIs. Per sample, six ROIs were selected within the tumor area, three with low immune cell infiltration and three with high immune cell infiltration.

After hybridization of probes to slide-mounted FFPE tissue sections, the oligonucleotide tags were released from the tissue ROIs via ultraviolet radiation exposure. Released tags were quantitated in a standard nCounter assay (NanoString Technologies).

**DNA and RNA sequencing.** DNA and RNA were extracted from fresh-frozen pretreatment tumor material using the AllPrep DNA/RNA Kit (QIAGEN) for frozen material, following manufacturer's protocol, in a QIAcube (QIAGEN). Germline DNA was isolated from each patient's peripheral blood mononuclear cells using the DNeasy Blood & Tissue Kit (QIAGEN). Analyses were performed for 18 patients; 2 patients (one in each arm) could not be analyzed because there were not enough tumor cells in the frozen biopsy to isolate DNA and RNA.

Strand-specific libraries were generated using the TruSeq Stranded mRNA Sample Prep Kit (Illumina) according to the manufacturer's instructions. Briefly, polyadenylated RNA from intact total RNA was purified using oligo-dT beads. Following purification, the RNA was fragmented, random primed, and reverse transcribed using SuperScript II Reverse Transcriptase (Thermo Fisher Scientific) with the addition of dactinomycin. Second strand synthesis was performed using polymerase I and RNaseH, replacing deoxythymidine triphosphate with deoxyuridine triphosphate. The generated complementary DNA fragments were 3' end adenylated and ligated to Illumina paired-end sequencing adapters and subsequently amplified by 12 cycles of PCR. The libraries were analyzed on a 2100 Bioanalyzer using a 7500 chip (Agilent), diluted, and pooled equimolar into a multiplex sequencing pool and stored at –20 °C. The libraries were sequenced with 65 base pair (bp) single-end reads on a HiSeq 2500 System in high output mode using V4 chemistry (Illumina). Raw reads were aligned to GRCh38 using a STAR RNA-seq aligner (see URLs) after which gene expression levels were quantified by Salmon (see URLs) using default parameters for both applications.

DNA was fragmented to 200–300-bp fragments by Covaris DNA shearing, after which library preparation was performed using KAPA HTP/LTP DNA Library Kit (Roche), according to manufacturer's instructions. Subsequently, exome enrichment was performed using the SureSelect XT2 Human All Exon v6 kit (Agilent) according to the manufacturer's instructions. The libraries were sequenced with 100-bp paired-end reads on a HiSeq 2500 in rapid run mode using V2 chemistry, with a median sequencing depth of 84-fold (range: 49,111). Raw reads were aligned to GRCh38 using the Burrows–Wheeler Aligner (see URLs), followed by the marking of duplicate reads by PicardMarkDuplicates and indel realignment by IndelRealigner (GATK; see URLs). Subsequently, base quality scores were recalibrated using BaseRecalibrator (GATK; see URLs) and variants were called using SomaticSniper (see URLs) and IndelGenotyper (GATK) for single nucleotide variants (SNVs) and indels, respectively. Non-synonymous mutational load was determined by summation of coding SNVs and frameshifting indels. Tumor transcripts were reconstructed using the identified SNVs and indels, and candidate tumor-specific neo-antigens were determined. We annotated candidate neo-antigens using our in-house epitope prediction pipeline that models the major prerequisites for (neo-)antigen presentation: RNA expression level; proteasomal processing and human leukocyte antigen binding. All epitopes passing filtering were subsequently used in combinatorial coding neo-antigen screens.

**MHC tetramer staining.** Neo-peptides as well as ultraviolet radiation cleavable peptides were synthesized as described previously<sup>32</sup>. Specific peptide-MHC complexes were generated by ultraviolet-induced ligand exchange in a 384-well format. In brief, pMHC complexes loaded with ultraviolet-sensitive peptide (100 μg ml<sup>-1</sup>) were subjected to 366 nm ultraviolet light (CAMAG) for 1 h at 4 °C in

the presence of rescue peptide (200  $\mu\text{M}$ ). pMHC multimers were generated using a total of ten different fluorescent streptavidin (SA) conjugates (Invitrogen). For each 10  $\mu\text{l}$  of pMHC monomer (100  $\mu\text{g ml}^{-1}$ ), the following amount of SA conjugates was added: 1.25  $\mu\text{l}$  SA-QD585; 1.5  $\mu\text{l}$  SA-QD605; 1.0  $\mu\text{l}$  SA-QD625; 1.5  $\mu\text{l}$  SA-QD655; 1.5  $\mu\text{l}$  SA-QD705; 1.0  $\mu\text{l}$  SA-QD800; 1.1  $\mu\text{l}$  SA-PE (1  $\text{mg } \mu\text{l}^{-1}$ ); 1.1  $\mu\text{l}$  SA-Cy7-PE (1  $\text{mg } \mu\text{l}^{-1}$ ); 0.4  $\mu\text{l}$  SA-BV421; 0.75  $\mu\text{l}$  PerCP-eFlour 710; and 0.6  $\mu\text{l}$  SA-APC (1  $\text{mg } \mu\text{l}^{-1}$ ). For each pMHC monomer, conjugation was performed with two of these fluorochromes. Mixtures were incubated for 30 min on ice.  $\text{NaN}_3$  (0.02% wt/vol) and an excess of D-biotin (26.4 mM; Sigma-Aldrich) was added to block residual binding sites.

For T cell staining, the pMHC multimer panels were collected and centrifuged at 4  $^{\circ}\text{C}$  for 2 min at 10,000g. The cells were stained for 15 min at 37  $^{\circ}\text{C}$ . Subsequently, 2  $\mu\text{l}$  anti-CD8-Alexa Fluor 700, 1  $\mu\text{l}$  anti-CD4-fluorescein isothiocyanate (FITC), 1  $\mu\text{l}$  anti-CD14-FITC, 1  $\mu\text{l}$  anti-CD16-FITC, 3  $\mu\text{l}$  anti-CD19-FITC, and 0.5  $\mu\text{l}$  LIVE/DEAD Fixable Near-IR Dead Cell Stain Kit (Thermo Fisher Scientific) were added for 20 min incubation on ice. Before flow cytometric analysis, cells were washed twice.

Data acquisition was performed on an LSR-II flow cytometer (BD Biosciences) with FACSDiva (v7) software. To identify antigen-specific T cells, the following gating strategy was used: (1) selection of live (IRDye dim) single-cell lymphocytes (forward scatter-width/height: low; side scatter-width/height: low; forward/side scatter-area); (2) selection of anti-CD8-AF700 $^{+}$  and 'dump' (anti-CD4, anti-CD14, anti-CD16, anti-CD19) negative cells; (3) selection of CD8 $^{+}$  T cells that were positive in two and only two MHC multimer channels. Cutoff values for the definition of positive responses were  $\geq 0.005\%$  of total CD8 $^{+}$  cells and  $\geq 10$  events. All responses were confirmed in independent experiments, using a different fluorochrome combination. Due to the sensitivity of the assay, the magnitude of T cell response is listed with four digits; this does not reflect the precision of detection. To monitor the reproducibility of the assay system, reference samples with four known T cell responses present at varying frequencies were included in each analysis.

Detected neoantigen responses were followed over time in peripheral blood to establish the kinetics of the detected responses. For this purpose, antigen-specific T cell responses were stained as described for the neo-antigen screens.

**Reporting summary.** Further information on research design is available in the Nature Research Reporting Summary linked to this article.

### Data availability

The RNA and DNA sequencing datasets generated during the current study have been deposited into the European Genome-phenome Archive under accession number [EGAS00001003099](https://www.ebi.ac.uk/ena/browser/view/EGAS00001003099) and are available on request. Every request will be reviewed by the institutional review board of the NKI; the researcher will need to sign a data access agreement with the NKI after approval. The TCR sequencing data that support the findings of this study are available from Adaptive Biotechnologies; however, restrictions apply to the availability of these data, which were used under license for the current study and so are not publicly available. However, data are available from the authors on reasonable request and with the permission of Adaptive Biotechnologies. The DSP data that support the findings of this study are available from NanoString; however, restrictions apply to the availability of these data, which were used under license for the current study and so are not publicly available. However, data are available from the authors on reasonable request and with permission from NanoString.

### References

- Robins, H. S. et al. Comprehensive assessment of T-cell receptor beta-chain diversity in alphabeta T cells. *Blood* **114**, 4099–4107 (2009).
- Carlson, C. S. et al. Using synthetic templates to design an unbiased multiplex PCR assay. *Nat. Commun.* **4**, 2680 (2013).
- Robins, H. et al. Ultra-sensitive detection of rare T cell clones. *J. Immunol. Methods* **375**, 14–19 (2012).
- Toebe, M. et al. Design and use of conditional MHC class I ligands. *Nat. Med.* **12**, 246–251 (2006).

## Reporting Summary

Nature Research wishes to improve the reproducibility of the work that we publish. This form provides structure for consistency and transparency in reporting. For further information on Nature Research policies, see [Authors & Referees](#) and the [Editorial Policy Checklist](#).

### Statistical parameters

When statistical analyses are reported, confirm that the following items are present in the relevant location (e.g. figure legend, table legend, main text, or Methods section).

n/a Confirmed

- The exact sample size ( $n$ ) for each experimental group/condition, given as a discrete number and unit of measurement
- An indication of whether measurements were taken from distinct samples or whether the same sample was measured repeatedly
- The statistical test(s) used AND whether they are one- or two-sided  
*Only common tests should be described solely by name; describe more complex techniques in the Methods section.*
- A description of all covariates tested
- A description of any assumptions or corrections, such as tests of normality and adjustment for multiple comparisons
- A full description of the statistics including central tendency (e.g. means) or other basic estimates (e.g. regression coefficient) AND variation (e.g. standard deviation) or associated estimates of uncertainty (e.g. confidence intervals)
- For null hypothesis testing, the test statistic (e.g.  $F$ ,  $t$ ,  $r$ ) with confidence intervals, effect sizes, degrees of freedom and  $P$  value noted  
*Give  $P$  values as exact values whenever suitable.*
- For Bayesian analysis, information on the choice of priors and Markov chain Monte Carlo settings
- For hierarchical and complex designs, identification of the appropriate level for tests and full reporting of outcomes
- Estimates of effect sizes (e.g. Cohen's  $d$ , Pearson's  $r$ ), indicating how they were calculated
- Clearly defined error bars  
*State explicitly what error bars represent (e.g. SD, SE, CI)*

*Our web collection on [statistics for biologists](#) may be useful.*

### Software and code

Policy information about [availability of computer code](#)

Data collection

BD FACSDIVA (v7)

Data analysis

BD FACSDIVA (v7); FlowJo (v10); R (v3.3.1); GraphPad Prism (v7.03); Adaptive ImmunoSEQ analyzer (v3); bwa-mem (v0.7); Picard (v2.10); somaticSniper (v1.0.5.0); GATK (v2.3); STAR RNAseq aligner (v2.5.3); Salmon (v0.8.2)

For manuscripts utilizing custom algorithms or software that are central to the research but not yet described in published literature, software must be made available to editors/reviewers upon request. We strongly encourage code deposition in a community repository (e.g. GitHub). See the Nature Research [guidelines for submitting code & software](#) for further information.

### Data

Policy information about [availability of data](#)

All manuscripts must include a [data availability statement](#). This statement should provide the following information, where applicable:

- Accession codes, unique identifiers, or web links for publicly available datasets
- A list of figures that have associated raw data
- A description of any restrictions on data availability

The RNA and DNA sequencing datasets generated during the current study have been deposited into European Genome-phenome Archive under accession EGAS00001003099 and are available upon request. Every request will be reviewed by the institutional review board of the NKI and the researcher needs to sign a

data access agreement with the NKI after approval. The TCR sequencing data that support the findings of this study are available from Adaptive Biotechnologies but restrictions apply to the availability of these data, which were used under license for the current study, and so are not publicly available. Data are however available from the authors upon reasonable request and with permission of Adaptive Biotechnologies. The DSP data that support the findings of this study are available from NanoString but restrictions apply to the availability of these data, which were used under license for the current study, and so are not publicly available. Data are however available from the authors upon reasonable request and with permission of NanoString.

## Field-specific reporting

Please select the best fit for your research. If you are not sure, read the appropriate sections before making your selection.

Life sciences  Behavioural & social sciences  Ecological, evolutionary & environmental sciences

For a reference copy of the document with all sections, see [nature.com/authors/policies/ReportingSummary-flat.pdf](https://nature.com/authors/policies/ReportingSummary-flat.pdf)

## Life sciences study design

All studies must disclose on these points even when the disclosure is negative.

Sample size	The primary endpoint of the study is in particular the safety and feasibility of intermittent surgery during immunotherapy with nivolumab plus ipilimumab (neo-adjuvant arm). This needs to be contrasted to a therapy where the combination is given as adjuvant therapy (also experimental). The optimal way to gain experience with these approaches is by randomizing in a phase 1b design. We therefore proposed to randomize 20 patients to either receiving the combination of ipilimumab + nivolumab adjuvant, or to split neo-adjuvant and adjuvant with surgery in between (10 patients per arm). The study was defined as not safe and feasible, if 2 out of the first 5 patients (point estimate 0.4 (95%CI 0.05-0.85)) or 4 out of the 10 (point estimate 0.4 (95%CI 0.12-0.74)) patients in the neo-adjuvant arm would have experienced immune-related adverse events leading to delayed surgery (not performed during week 6) or experience grade 3/4 SUSARs after surgery, that are attributed to the pre-surgery immunotherapy. The investigators realized that numbers of immune-related adverse events smaller than respectively 2 and 4 still bare a substantial chance of error of taking the wrong conclusion about safety. The number of ten patients in each arm is chosen with the focus on producing relevant numbers of T cell responses that can be analyzed (immune-activating capacity). In patients with metastatic melanoma, neo-antigen specific T cell responses are observed in the majority of patients (>75%) by the technology used.
Data exclusions	Patients were only excluded if they did not meet the pre-defined inclusion and exclusion criteria of the study protocol (see Supplementary Material for all inclusion and exclusion criteria). Eligible patients were 18 years of age or older with histologically confirmed resectable stage III melanoma with palpable lymph node metastases and no history of in-transit metastases within the last 6 months. A World Health Organization (WHO) Performance Status of 0 or 1, and normal lactate dehydrogenase (LDH) levels were required. Exclusion criteria included autoimmune disease, HIV or hepatitis B or C infection, prior immunotherapy targeting CTLA-4, PD-1 or PD-L1, immunosuppressive medications within 6 months prior to study inclusion, and radiotherapy prior or post-surgery within the trial.
Replication	Experimental replicates were not attempt and were not applicable for our study.
Randomization	Patients were randomized by the independent trial office of the NKI
Blinding	No blinding was performed as it is not ethical to give neoadjuvant placebo therapy and thereby postponing active surgical treatment.

## Reporting for specific materials, systems and methods

### Materials & experimental systems

n/a	Involved in the study
<input checked="" type="checkbox"/>	<input type="checkbox"/> Unique biological materials
<input type="checkbox"/>	<input checked="" type="checkbox"/> Antibodies
<input checked="" type="checkbox"/>	<input type="checkbox"/> Eukaryotic cell lines
<input checked="" type="checkbox"/>	<input type="checkbox"/> Palaeontology
<input checked="" type="checkbox"/>	<input type="checkbox"/> Animals and other organisms
<input type="checkbox"/>	<input checked="" type="checkbox"/> Human research participants

### Methods

n/a	Involved in the study
<input checked="" type="checkbox"/>	<input type="checkbox"/> ChIP-seq
<input type="checkbox"/>	<input checked="" type="checkbox"/> Flow cytometry
<input checked="" type="checkbox"/>	<input type="checkbox"/> MRI-based neuroimaging

## Antibodies

### Antibodies used

Antibodies used for flow cytometry (clone):  
 Anti-CD8 Alexa-fluor700 (RPA-T8, 557945), anti-CD4-FITC (SK3), anti-CD14-FITC (MφP9), anti-CD16-FITC (NKP15), anti-CD19-FITC (4G7) were purchased from BD. LIVE/DEAD Fixable Near-IR Dead cell stain kit was purchased from Invitrogen.  
 Antibodies used for IHC to define ROI for NanoString DSP analysis:

Anti-S100B-dylight 550 (15F4NB) purchased from Novus, anti-CD45-AlexaFluor647 (D9M81) purchased from Cell Signalling Technology, Syto83 (S11364) purchased from Thermofisher.

Validation

All antibodies are commercially available and were only used for applications validated by the manufacturer

## Human research participants

Policy information about [studies involving human research participants](#)

Population characteristics

20 stage III melanoma patients with palpable disease were included in the study, 65% were male and median age was 54 years. Detailed patient characteristics per treatment arm are described in table 1.

Recruitment

All patients with palpable stage III disease were offered to participate in this trial.

## Flow Cytometry

Plots

Confirm that:

- The axis labels state the marker and fluorochrome used (e.g. CD4-FITC).
- The axis scales are clearly visible. Include numbers along axes only for bottom left plot of group (a 'group' is an analysis of identical markers).
- All plots are contour plots with outliers or pseudocolor plots.
- A numerical value for number of cells or percentage (with statistics) is provided.

Methodology

Sample preparation

Specific peptide-MHC complexes were generated by UV-induced ligand exchange in a 384 well format. In brief, pMHC complexes loaded with UV-sensitive peptide (100µg ml<sup>-1</sup>) were subjected to 366 nm UV light (Camag) for 1h at 4°C in the presence of rescue peptide (200µM). pMHC multimers were generated using a total of 10 different fluorescent streptavidin (SA) conjugates (Invitrogen). For each 10µl of pMHC monomer (100µg ml<sup>-1</sup>), the following amount of SA-conjugates was added: 1.25µl SA-QD585, 1.5µl SA-QD605, 1.0µl SA-QD625, 1.5µl SA-QD655, 1.5µl SA-QD705, 1.0µl SA-QD800, 1.1µl SA-PE (1 mg µl<sup>-1</sup>), 1.1µl SA-Cy7-PE (1 mg µl<sup>-1</sup>), 0.4µl SA-BV421, 0.75µl PerCP-eFlour710 and 0.6µl SA-APC (1mg µl<sup>-1</sup>). For each pMHC monomer, conjugation was performed with two of these fluorochromes. Mixtures were incubated 30 min on ice. Na<sub>3</sub>N (0.02% wt/vol) and an excess of D-biotin (26.4mM, Sigma) was added to block residual binding sites. For T cell staining, the pMHC multimer panels were collected and centrifuged at 4°C for 2min at 10.000g. The cells were stained for 15 min at 37 °C. Subsequently, 2 µl anti-CD8-Alexa-fluor700, 1 µl anti-CD4-FITC, 1 µl anti-CD14-FITC, 1 µl anti-CD16-FITC, 3 µl anti-CD19-FITC and 0.5 µl LIVE/DEAD® Fixable IR Dead Cell Stain Kit were added for 20 min incubation on ice. Before flow cytometric analysis, cells were washed twice.

Instrument

LSR-II flow cytometer (BD)

Software

BD FACSDIVA (v7), FlowJo (v10)

Cell population abundance

n.a.

Gating strategy

To identify antigen-specific T cells, the following gating strategy was (i) Selection of live (IR-dye dim) single cell lymphocytes (FSC-W/H low, SSC-W/H low, FSC/SSC-A). (ii) Selection of anti-CD8-AF700+ and 'dump' (anti-CD4, -CD14, -CD16, -CD19) negative cells. (iii) Selection of CD8+ T cells that were positive in two and only two MHC multimer channels. Cut off values for the definition of positive responses were > 0.005% of total CD8+ cells and >10 events. All responses were confirmed in independent experiments, using a different fluorochrome combination.

- Tick this box to confirm that a figure exemplifying the gating strategy is provided in the Supplementary Information.